



Originally published as:

Yaroshenko, V., Lühr, H. (2018): Reversed Hall effect and plasma conductivity in the presence of charged impurities. - *Physics of Plasmas*, 25.

DOI: <http://doi.org/10.1063/1.5012691>

## Reversed Hall effect and plasma conductivity in the presence of charged impurities

V. V. Yaroshenko and H. Lühr

*GFZ German Research Center For Geosciences, Telegrafenberg, 14473 Potsdam, Germany*

(Received 7 November 2017; accepted 30 December 2017; published online 10 January 2018)

The Hall conductivity of magnetized plasma can be strongly suppressed by the contribution of negatively charged particulates (referred further as “dust”). Once the charge density accumulated by the dust exceeds a certain threshold, the Hall component becomes negative, providing a reversal in the Hall current. Such an effect is unique for dust-loaded plasmas, and it can hardly be achieved in electronegative plasmas. Further growth of the dust density leads to an increase in both the absolute value of the Hall and Pedersen conductivities, while the field-aligned component is decreased. These modifications enhance the role of transverse electric currents and reduce the anisotropy of a magnetized plasma when loaded with charged impurities. The findings provide an important basis for studying the generation of electric currents and transport phenomena in magnetized plasma systems containing small charged particulates. They can be relevant for a wide range of applications from naturally occurring space plasmas in planetary magnetospheres and astrophysical objects to laboratory dusty plasmas (Magnetized Dusty Plasma Experiment) and to technological and fusion plasmas. *Published by AIP Publishing.* <https://doi.org/10.1063/1.5012691>

The electric conductivity of magnetized plasma plays a major role in many various physical phenomena in laboratory, space, and astrophysical plasmas. We mention only a few basic implications of this concept. The plasma conductivity is strongly related to the self-consistent electric field structures and problems of the plasma stability which are of high priority in various laboratory and fusion devices.<sup>1</sup> In the near-Earth environment, it is of importance for understanding the atmospheric electricity phenomena, i.e., an interdisciplinary topic, involving concepts from electrostatics, atmospheric physics, meteorology, and Earth science.<sup>2,3</sup> The plasma conductivity plays a fundamental role in the ionospheric physics: it is strongly related to the self-consistent electric field-current system existing in the Earth’s ionosphere and closure the field-aligned currents, determines the Joule heating, and is a key issue for the atmosphere-ionosphere-magnetosphere interaction.<sup>4</sup> In astrophysical plasmas, the plasma conductivity influences the magnetic field line reconnection and can lead to the so-called “reconnection diffusion” which is believed to play a crucial role in flare physics and star formation.<sup>5,6</sup>

Most published works considering the conductivity problem, however, deal either with weakly ionized electron-ion plasmas where the plasma particle-neutral collisions dominate (neglecting the Coulomb collisions) or with fully ionized plasmas, in which the role of neutral collisions is negligible. On the other hand, there is a class of weakly ionized plasmas, the so-called dusty plasma, where both kinds of collisional processes can be on an equal footing.<sup>7</sup> Since such a combination of conventional plasma and fine solid particles is ubiquitous in space (e.g., molecular clouds, comet tails, ring systems of the giant planets, and Earth’s mesosphere),<sup>8</sup> an examination of the dust effect on the plasma conductivity is required. Furthermore, some previous studies indicate interesting consequences of the presence of charged dust particles associated with the plasma

conductivity. In particular, modification of the Hall conductivity by the immobile micron-sized dust in the co-rotating plasma flow near Saturn’s moon Enceladus (in the so-called plume region) reported in Ref. 9 can provide a negative Hall current. The latter has been invoked for the explanation of the magnetic field perturbations registered by the Cassini magnetometer in the plume region.<sup>9–11</sup> Recently, Yaroshenko and Lühr<sup>12,13</sup> analyzed self-consistently the dynamics of negatively charged nano-sized grains (a major dust component of the moon’s plume<sup>14</sup>) considering them as additional plasma species to rework the plasma conductivity. A novel condition of the reversed Hall effect has been derived, and significant modifications of the conductivity components in the Enceladus plume plasma have been predicted.<sup>13</sup> The influence of various models of grain populations of dense molecular clouds on the plasma conductivity tensor has also been considered with a special emphasis on the role of the Hall term on the magnetic field evolution and Hall diffusion.<sup>15–17</sup> Variations of the plasma conductivity along the magnetic field due to the sedimentation of charged dust are predicted to lead to the existence of a large vertical electric field at mesospheric altitudes.<sup>18</sup>

Although some specific aspects of the dust influence on the electric conductivity have been discussed before, we believe that it is timeous to consider this issue in general, especially keeping in mind the wide range of its application. In this letter, therefore, we report on modifications of the conductivity tensor due to the presence of charged particulates which are considered as a plasma species. The approach includes particle collisions with neutral gas and exchange of momentum transfer between plasma and charged dust species. Our findings are quite unusual for conventional magnetized plasmas and might have interesting consequences for many space and laboratory plasma conditions. Below, we show the relevance of the reversed Hall effect and the

increase in the Pedersen conductivity and suppression of the parallel conductivity in laboratory [Magnetized Dusty Plasma Experiment (MDPX)<sup>19,20</sup>] and space plasmas.

Table I gives average characteristics for some natural and laboratory plasmas containing negatively charged particulates which can be used for the illustration of our results. Here, we also provide the number of charged grains in the Debye sphere—the dust plasma parameter  $N$ . In all cases,  $N \gg 1$ , and hence, the charged dust particles can be considered as additional plasma species. Furthermore, Table I contains the values of the standard Hall parameter defined as a ratio of the gyro-frequency to the collisional frequency of the plasma particles with neutrals ( $\eta_{\alpha 0} = \omega_{B\alpha}/\nu_{\alpha n}$  with  $\alpha = e, i, \text{ and } d$ ). Therefore, the Hall parameter describes the number of gyro periods between two collisions with neutrals, and the condition  $\eta_{\alpha 0} \gg 1$  means a high degree of magnetization of the  $\alpha$  species in a conventional plasma. As seen in various dusty plasmas, it is possible to find plasma states where only the electrons, electrons, and ions and even all three charged plasma species including the dust particles are magnetized.

When plasmas are embedded in a magnetic field, the current does not only flow parallel to the applied electric field; rather, the relationship between the current density  $\mathbf{j}$  and electric field  $\mathbf{E}$  is expressed in terms of a tensor conductivity  $\mathbf{J} = \hat{\sigma}\mathbf{E}$ , viz.,

$$\mathbf{J} = \sigma_{\parallel}\mathbf{E}_{\parallel} + \sigma_H B_0^{-1}[\mathbf{B}_0 \times \mathbf{E}_{\perp}] + \sigma_P \mathbf{E}_{\perp}, \quad (1)$$

where  $\mathbf{E}_{\parallel}$  and  $\mathbf{E}_{\perp}$  are the components of the electric field parallel and perpendicular to the ambient magnetic field,  $\mathbf{B}_0$ . Quantities, determining the transverse ( $\perp \mathbf{B}_0$ ) currents, are the Hall,  $\sigma_H$ , and Pedersen,  $\sigma_P$ , components, while the parallel conductivity,  $\sigma_{\parallel}$ , is responsible for the current along  $\mathbf{B}_0$ . Using the formalism developed in Ref. 13, we deduce the conductivity elements taking into account particle collisions with neutrals and plasma-dust interactions. This approach treats all the species, i.e., the electrons, ions, and charged particulates, in the conventional fluid approximation. For simplicity, the grains are assumed to be mono-disperse, having fixed negative charges and controlled mainly by electromagnetic forces. The latter assumption is typically valid for nanometer-sized grains in space conditions (see, e.g., Ref.

13). For strong magnetic fields, employed in MDPX plasmas, the domination of the electromagnetic forces requires sub-micron grain sizes.<sup>20</sup>

The presence of dust influences the plasma conductivity in several ways. The first obvious effect is that the dust charging reduces the ambient electron density and hence diminishes the electron contribution to the conductivity components. An electron depletion is expressed in terms of the Havnes parameter  $p = Z_d n_d / n_i$  through

$$n_e = n_i(1 - p), \quad (2)$$

where  $n_{\alpha}$  denotes the density of different plasma species,  $\alpha = e, i, \text{ and } d$ , and dust charge is  $q_d = eZ_d$ . Second, the plasma-dust interaction can significantly change the ion Hall parameter,  $\eta_i = \omega_{Bi}/\nu_i$ , which now involves the net collisional frequency of ions with neutrals,  $\nu_{in}$ , and dust particles,  $\nu_{id}$ , namely,  $\nu_i = \nu_{in} + \nu_{id}$ . The quantity  $\nu_{id}$  is a strong function of grain charge and dust density, and it might easily be of the same order of magnitude as  $\nu_{in}$ .<sup>7,13,23,24</sup> Finally, the conductivity components contain additional terms associated with charged grains whose impact depends on the value of  $p$  and the dust Hall parameter  $\eta_d = \omega_{Bd}/\nu_d$ , where the quantity  $\nu_d$  in a similar way defines the net collisional frequency through  $\nu_d = \nu_{dn} + \nu_{di}$ . In most weakly ionized dusty plasmas, however, the dust-neutral collisional frequency significantly dominates over the dust-ion collisional frequency, i.e.,  $\nu_{di} \ll \nu_{dn}$ , because of  $n_i \ll n_n$ , and thus,  $\nu_{di}$  can be neglected as a good approximation, leading to  $\nu_d \simeq \nu_{dn}$  and hence  $\eta_d \simeq \eta_{d0} = \omega_{Bd}/\nu_{dn}$ . The interplay between  $p$ ,  $\eta_d$ , and  $\eta_i$  determines the final form of the conductivity tensor components in the presence of charged particulates.<sup>13</sup> In the case of magnetized electrons  $\eta_e \gg 1$ , they can be written as

$$\sigma_H = \sigma_{H0} \frac{(1 + \eta_{i0}^2)}{(1 + \eta_{d0}^2)} (p_{cr} - p), \quad (3)$$

$$\sigma_P = \sigma_{P0} \frac{(1 + \eta_{i0}^2)\nu_{in}}{(1 + \eta_{d0}^2)\nu_i} \left( p_{cr} + \frac{\eta_{d0}}{\eta_i} \left( p - \frac{\nu_{id}}{\nu_i} \right) \right), \quad (4)$$

$$\sigma_{\parallel} = \sigma_{\parallel 0} \left( 1 - p + \frac{\eta_i - \left( \frac{\nu_{id}}{\nu_i} - p \right) \eta_{d0}}{\eta_{e0}} \right). \quad (5)$$

TABLE I. Characteristics of dusty plasmas.<sup>a</sup>

Parameter	Symbol	MDPX	Plume	Mesosphere	Molecular cloud
Plasma density (cm <sup>-3</sup> )	$n_0$	10 <sup>9</sup> –10 <sup>10</sup>	10 <sup>2</sup> –10 <sup>3</sup>	10 <sup>2</sup> –10 <sup>3</sup>	10 <sup>-4</sup> –10 <sup>-1</sup>
Electron temperature (eV)	$T_e$	2–5	1	≥0.01	≥0.003
Neutral gas density (cm <sup>-3</sup> )	$n_n$	10 <sup>14</sup> –10 <sup>15</sup>	10 <sup>6</sup> –10 <sup>9</sup>	10 <sup>13</sup> –10 <sup>14</sup>	10 <sup>4</sup> –10 <sup>14</sup>
Particle size (nm)	$a$	~10 <sup>3</sup>	≥1	~1–30	≥5
Dust density (cm <sup>-3</sup> )	$n_d$	10 <sup>3</sup> –10 <sup>6</sup>	1–10 <sup>3</sup>	10 <sup>2</sup> –10 <sup>3</sup>	~10 <sup>-6</sup> –10 <sup>-1</sup>
Dust plasma parameter	$N$	10 <sup>2</sup>	10 <sup>4</sup> –10 <sup>7</sup>	10 <sup>4</sup> –10 <sup>5</sup>	10 <sup>5</sup> –10 <sup>6</sup>
Magnetic field (G)	$B_0$	≤4 × 10 <sup>4</sup>	3.25 × 10 <sup>-3</sup>	0.5	~10 <sup>-4</sup> –10 <sup>-1</sup>
Electron Hall parameter <sup>b</sup>	$\eta_{e0}$	10 <sup>2</sup> –10 <sup>3</sup>	10 <sup>4</sup> –10 <sup>6</sup>	≥10	10 <sup>7</sup> –1
Ion Hall parameter	$\eta_{i0}$	1–10	10–10 <sup>3</sup>	10 <sup>-2</sup>	10 <sup>4</sup> –10 <sup>-3</sup>
Dust Hall parameter	$\eta_{d0}$	≤5 × 10 <sup>-2</sup>	1–10 <sup>2</sup>	≤10 <sup>-3</sup>	≤10 <sup>3</sup> –10 <sup>-4</sup>

<sup>a</sup>Numerical data are adopted from Refs. 19 and 20: MDPX plasma,<sup>10,12,14</sup> Enceladus plume,<sup>21</sup> mesosphere,<sup>15</sup> and molecular gas with the MRN dust-size distribution.<sup>22</sup>

<sup>b</sup>Estimates of the Hall parameters correspond to respective maximal values of  $B_0$ .

The index 0 describes the appropriate components in the conventional electron-ion plasma ( $n_e = n_i = n_0$ ,  $\eta_{e0} \gg \eta_{i0}$ ):  $\sigma_{H0} \simeq \sigma_{\parallel 0}/(\eta_{e0}(1 + \eta_{i0}^2))$ ,  $\sigma_{P0} \simeq (\sigma_{\parallel 0}/\eta_{e0})(1/\eta_{e0} + \eta_{i0}/(1 + \eta_{i0}^2))$ , and  $\sigma_{\parallel 0} \simeq (en_0/B_0)\eta_{e0}$ . In the conventional plasma, the field-aligned term,  $\sigma_{\parallel 0}$ , solely determined by electrons moving freely along the field lines, is several orders of magnitude higher than the Pedersen and Hall elements. If the ions are also magnetized ( $\eta_{i0} > 1$ ), they obey the standard ordering  $\sigma_{\parallel 0} \gg \sigma_{P0} > \sigma_{H0}$ .

The transverse tensor components involve the quantity

$$p_{cr} = \frac{(1 + \eta_{d0}^2)}{1 + \eta_i^2} \left( 1 + \frac{\nu_{id} \eta_{d0} (\eta_i - \eta_{d0})}{\nu_i (1 + \eta_{d0}^2)} \right), \quad (6)$$

which is crucial for the Hall term: the plasma with  $p > p_{cr}$  ensures the reversed direction of the Hall current. Expression (6) represents the most general form of the threshold of the reversed Hall effect. Only some limiting cases of  $p_{cr}$  have been studied for the dust-loaded plume.<sup>13</sup> Now, we examine the critical value (6) to search for a parameter space, providing the negative Hall current in various dusty plasmas.

For MDPX conditions,  $\eta_{i0} \geq 1 \gg \eta_{d0}$ , and (6) yields  $p_{cr} \simeq (1 + A)^2 / ((1 + A)^2 + \eta_{i0}^2)$ , where the coefficient  $A = \nu_{id} \nu_{in}$  describes the relative contribution of ion-dust collisions. For many complex plasma experiments, a reasonable approximation for  $\nu_{id}$  is described by the model<sup>24</sup> valid when the ion-neutral mean free path is larger than the Coulomb radius of the ion-particle interaction and for small dust number density ( $p < 1$ ). In this case, the main contribution to the momentum transfer between ions and the dust particle is due to elastic ion scattering in the electric field of the grain. It leads often to  $A \sim 1$ , and therefore, the ion-dust Coulomb interactions could essentially increase the threshold value (6), which in the absence of Coulomb particle interactions ( $A = 0$ ) would be only  $p_{cr} \simeq 1/\eta_{i0}^2$ . In Fig. 1, we show the 3D variations of  $p_{cr}$  with dust and plasma densities calculated for the

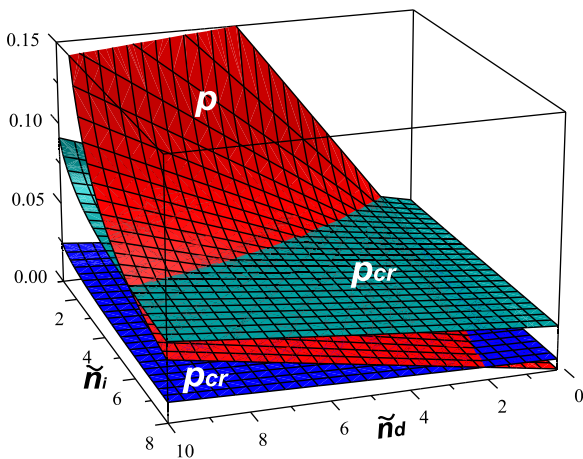


FIG. 1. Two surfaces (blue and blue-green online) express critical values  $p_{cr}$  at given “reduced” densities  $\tilde{n}_i = n_i/10^{-8} \text{ cm}^{-3}$  and  $\tilde{n}_d = n_d/10^4 \text{ cm}^{-3}$  for the conditions close to MDPX at magnetic field strengths  $B_0 = 2.5 \text{ T}$  and  $B_0 = 1.25 \text{ T}$ , respectively; in both cases, gas density  $n_n \sim 4 \times 10^{15} \text{ cm}^{-3}$ , electron and ion temperatures  $T_e = 2.5 \text{ eV}$  and  $T_i = 0.025 \text{ eV}$ , dust size  $a = 1 \mu\text{m}$ , charge  $Z_d = 2900$ , and ion-neutral cross section  $\sigma_{in} = 5 \times 10^{-15} \text{ cm}^2$  are chosen according to Ref. 20. The third (red online) surface represents respective variations of the Havnes parameter  $p = Z_d n_d n_i$ .

two magnetic fields  $B_0 = 1.25 \text{ T}$  and  $B_0 = 2.5 \text{ T}$  and typical discharge parameters employed in the MDPX conditions.<sup>19,20</sup> The plasma density at various levels of RF-power is varied in the range of  $10^9 \leq n_i \leq 8 \times 10^9 \text{ cm}^{-3}$ . For the dust number density, we adopt values widely employed in complex plasma experiments ranging between  $2 \times 10^3 \leq n_d \leq 10^5 \text{ cm}^{-3}$ .

Figure 1 indicates the existence ranges in the parameter space  $\{n_d, n_i\}$ , where the admissible  $p$  lies above the upper ( $B = 1.25 \text{ T}$ ) and the lower ( $B = 2.5 \text{ T}$ ) surfaces expressing  $p_{cr}$ , thus providing the reversed Hall effect in discharge plasmas. For example, for the lower limiting value of the plasma density  $n_i \sim 2 \times 10^9 \text{ cm}^{-3}$ , crossover between the curves  $p_{cr}$  and  $p$  occurs for small dust population,  $n_{dcr} \simeq 5 \times 10^3 \text{ cm}^{-3}$  ( $B = 2.5 \text{ T}$ ) and  $n_{dcr} \simeq 2.4 \times 10^4 \text{ cm}^{-3}$  ( $B = 1.25 \text{ T}$ ), leading to  $\sigma_H < 0$  for  $n_d > n_{dcr}$ . An increase in the plasma density to the upper limit  $n_i \sim 8 \times 10^9 \text{ cm}^{-3}$  requires higher critical densities  $n_{dcr} \simeq 2.1 \times 10^4 \text{ cm}^{-3}$  ( $B = 2.5 \text{ T}$ ) and  $n_{dcr} \simeq 2 \times 10^5 \text{ cm}^{-3}$  ( $B = 1.25 \text{ T}$ ), respectively. Since the densities  $n_d \sim 10^4 - 10^5 \text{ cm}^{-3}$  are commonly used in laboratory complex plasma studies, the negative Hall currents can ultimately influence the discharge structure. Clearly, the efficiency of the reversed Hall effect is significantly dependent on the RF-power, magnetic field strength, and dust characteristics.

Interestingly, the expression (6) strongly restricts the possibility of the reversed Hall effect in magnetized electro-negative plasmas. Introducing a fraction of negative ions with respect to the positive ones,  $p_i = n_{in}/n_i$ , we note that by definition  $p_i \leq 1$ . On the other hand, neglecting the Coulomb collisions ( $A \simeq 0$ ) in (6) yields  $p_i > (1 + \eta_{i_n}^2)/(1 + \eta_{i0}^2)$ , where the subscript  $i_n$  denotes the respective quantities for negative ions. Assuming that positive and negative ions are identical leads to the unrealistic limit  $p_i > 1$ . Solely, when  $\eta_{i0} > \eta_{i_n}$  (this can be reduced to the requirement of a large mass difference between the positive and negative ions,  $m_i < m_{i_n}$ ) combined with the condition that at least the positive ions are magnetized ( $\eta_{i0} > 1$ ) ensures  $p_i < 1$ , thus establishing highly specific conditions for the appearance of negative  $\sigma_H$ .

Contrary to complex plasma experiments, where for heavy particles  $\eta_{d0} \ll 1$ , the most numerous cosmic grains are typically small (nano-sized) and often ensure  $\eta_{d0} \geq 1$ . Hence, in space plasmas, one has to analyze the general expression (6). Figure 2(a) illustrates calculations of the threshold value  $p_{cr}$  (solid curves) and the Havnes parameter  $p$  (dashed curves) based on the data obtained by various Cassini instruments during a 1-min interval surrounding the E3 and E5 southward-encounters with the most dense part of the Enceladus plume.<sup>14</sup> The temporal evolutions of  $p_{cr}$  and  $p$  certainly admit regions where  $p > p_{cr}$  and hence  $\sigma_H < 0$  near the peak of the nanograin flux. The respective spacecraft velocity in the moon frame of reference, 14.4 km/s (E3) and 17.7 km/s (E5), yields the southward scale of such a region  $\sim 500 \text{ km}$ . Since the effects of charged dust, plasma particles, and electric conductivity are interrelated locally, the problem of the accompanied magnetic field perturbations appearing in these regions and the comparison with the respective Cassini magnetometer measurements becomes much more involved than the simplified model suggested in Ref. 9.

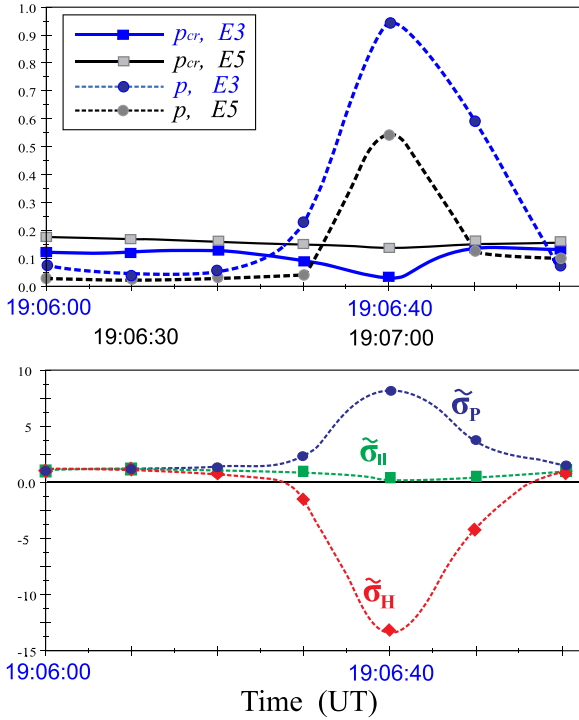


FIG. 2. (a) Temporal variations of  $p_{cr}$  during the 1-min interval surrounding the Cassini encounters with the dust-densest part of the Enceladus plume: E3-flyby (closest approach at 19:06:40 UT) and E5 (19:07:00 UT), respectively. For calculations, the respective Cassini measurements of the water vapor density,  $n_m$ ,<sup>25</sup> the plasma density,  $n_i$ ,<sup>26</sup> and the nanograin number densities,  $n_d$ ,<sup>14</sup> have been used. In both cases, the ion-neutral cross section is  $\sigma_{in} \simeq 3 \times 10^{-15} \text{ cm}^2$  (Ref. 27) and the dust size  $a = 2 \text{ nm}$ , while the particle charge is estimated in the model of Refs. 28 and 29. The dashed curves indicate variations of the corresponding Havnes parameter  $p$  during E3 and E5 flybys. (b) Appropriate temporal variations of the normalized Hall ( $\tilde{\sigma}_H = \sigma_H/\sigma_{H0}$ ), Pedersen ( $\tilde{\sigma}_P = \sigma_P/\sigma_{P0}$ ), and parallel conductivity ( $\tilde{\sigma}_\parallel = \sigma_\parallel/\sigma_{\parallel 0}$ ) during the E3 encounter.

In view of the potentially large role of the plasma conductivity in various astrophysical plasmas, we test qualitatively the scenario of the reversed Hall effect in molecular clouds. We focus on the range of neutral gas densities  $10^9 \geq n_n \geq 10^4 \text{ cm}^{-3}$ , where the plasma electrons and ions typically dominate over the charged grains, and the term  $n_d$  is associated mainly with negatively charged dust independently of the grain-size distribution applied.<sup>15</sup> In Fig. 3, we plot the threshold value (6) and the respective Havnes

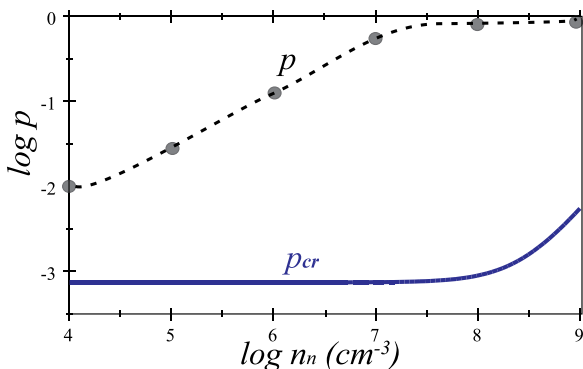


FIG. 3. Variations of the critical value  $p_{cr}$  and Havnes parameter  $p$  with the gas density in a molecular cloud for the MRN grain-size distribution.<sup>22</sup> The plasma species abundances are determined from Refs. 15 and 31.

parameter  $p$  for the MRN (Mathis-Rumpl-Nordsieck, Ref. 22) grain-size distribution  $dn_d = Cn_n a^{-3.5} da$ , with  $C = 1.5 \times 10^{-25} \text{ cm}^{-2.5}$ .<sup>30</sup> Such a distribution leads to a strong domination of the smallest grains  $a \sim 5 \text{ nm}$  which are typically singly charged. For the magnetic field model,  $B_0[\text{G}] = 10^{-3}(n_n[\text{cm}^{-3}]/10^6)^{1/2}$  at  $n_n < 10^6 \text{ cm}^{-3}$ ;  $B_0[\text{G}] = 10^{-3}(n_n[\text{cm}^{-3}]/10^6)^{1/4}$  at  $n_n > 10^6 \text{ cm}^{-3}$ , and the collisional frequencies of the plasma particles with neutrals as given in Ref. 15, one finds that the curve  $p_{cr}(n_n)$  remains always below the dependence  $p(n_n)$ , thus providing the condition for the reversed Hall currents in the whole range of gas densities. This result corroborates previous attempts to study the Hall term in dense molecular gas.<sup>15</sup>

The conductivity tensor components (3)–(5) in general exhibit new dependencies on magnetic field strength and gas and plasma densities because of the additional terms involving charged dust. Two illustrative examples are given in Figs. 2(b) and 4 to display the dust contribution to  $\sigma_H$ ,  $\sigma_P$ , and  $\sigma_\parallel$  through their comparison to the appropriate conventional forms. In the regime relevant for the laboratory complex plasma studies (Fig. 4), the normalized Pedersen term,  $\tilde{\sigma}_P = \sigma_P/\sigma_{P0}$ , grows slowly with the dust density almost replicating a dependence of the critical value  $p_{cr}$  vs.  $n_d$  (as shown in Fig. 1). Note that when the negative charge density accumulated by the dust species becomes of the same order as the ion density, i.e.,  $p \rightarrow 1$ , an upper limit of the Pedersen component would be determined mainly by the ion-dust Coulomb interactions, yielding  $\tilde{\sigma}_P \simeq (1 + A) > 1$ . Quite the contrary, the parallel conductivity at first order approximation is set by the electron depletion,  $\tilde{\sigma}_\parallel = \sigma_\parallel/\sigma_{\parallel 0} \propto (1 - p)$ , hence decreasing with the growth of  $n_d$ . In the limit  $p \rightarrow 1$ , the strongly reduced electron density would lead to  $\tilde{\sigma}_\parallel \ll 1$ . Figure 4 indicates that the Hall conductivity of the MDPX plasma can be also highly reduced  $\tilde{\sigma}_H = \sigma_H/\sigma_{H0} \ll 1$  at low dust population ( $n_d \lesssim n_{dcr} \sim 10^4 \text{ cm}^{-3}$ ). An increase in the dust density  $n_d > n_{dcr}$  causes the reversed Hall effect, and  $|\tilde{\sigma}_H|$  grows almost linearly with  $n_d$ . For realistic number densities  $n_d \gtrsim 10^5 \text{ cm}^{-3}$   $|\tilde{\sigma}_H|$  achieves factor of 10. As seen, the presence of a dust population in magnetized complex plasmas can therefore decrease the plasma anisotropy: while the field-aligned conductivity component is decreased, the

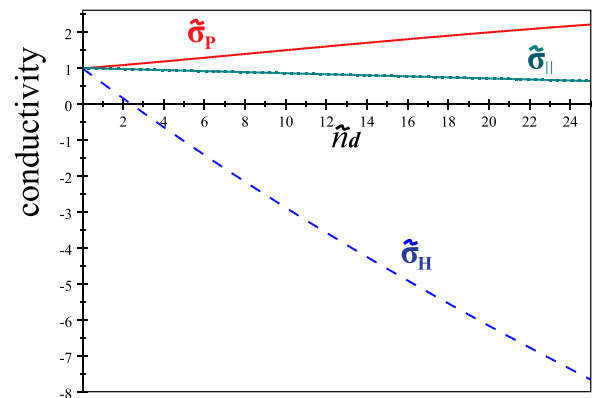


FIG. 4. Variations of the normalized Hall ( $\tilde{\sigma}_H = \sigma_H/\sigma_{H0}$ ), Pedersen ( $\tilde{\sigma}_P = \sigma_P/\sigma_{P0}$ ), and parallel conductivity ( $\tilde{\sigma}_\parallel = \sigma_\parallel/\sigma_{\parallel 0}$ ) with the dust density ( $\tilde{n}_d = n_d/10^4 \text{ cm}^{-3}$ ) for the MDPX plasmas at  $B_0 = 1.25 \text{ T}$  and plasma density  $n_0 = 2 \times 10^9 \text{ cm}^{-3}$ . Other parameters are as in Fig. 1.

absolute value of the Hall and the Pedersen conductivities can be considerably increased, providing a new ordering  $|\sigma_H| \geq \sigma_P$  and a smaller difference between the parallel and transverse tensor elements. A similar tendency can be found in temporal variations of the conductivities calculated during the 1-min interval surrounding the encounter E3 (19:06:40 UT), within the dust-densest part of the plume. Figure 2(b) shows a comparison between the elements (3)–(5) calculated from the Cassini dust/plasma measurements<sup>14,25,26</sup> and the respective values in the conventional plasma. Ignoring the charged grains in the plume plasma implies an order of magnitude smaller transverse tensor elements and two orders of magnitude higher parallel conductivity than those in the realistic case.

These theoretical results open up qualitatively new general properties of a magnetized plasma containing tiny negatively charged impurities, namely, the appearance of the reversed Hall effect even at small grain population, an increase in the transverse (with respect to the magnetic field) currents, and a simultaneous reduction of the parallel current with the growth of dust density. The reversed Hall effect has been supported by recent Cassini observations: the negative value of the Hall term explains the unusual orientation of the magnetic field perturbations detected by the magnetometer during close Enceladus flybys.<sup>9</sup> On the other hand, our estimates of the novel Hall and Pedersen elements based on the Cassini dust impact data in the dense plume surpass the respective values in the conventional plasma by a factor of 10, while the reduction of parallel conductivity reaches a factor of  $10^2$  (Fig. 2). Such a decrease in the plasma anisotropy by the plume nanograins can significantly influence available structures of Enceladus' Alfvén wings,<sup>9</sup> and the modeling of the Cassini magnetic field observations has to be adapted accordingly. In a similar way, one can expect local strong changes in the ionospheric conductivity due to the presence of numerous charged aerosol particles in Earth's polar mesosphere.<sup>21</sup> We anticipate that the footprints of the new electric conductivity could be manifested in the associated geomagnetic field perturbations. Their recognition in magnetometer data (at the ground level or in space) could further our knowledge about the polar mesospheric clouds. There is another consequence of our study that might be relevant for magnetized complex plasmas: invoking the plasma-dust Coulomb interactions essentially changes the transverse conductivity components and threshold value for the appearance of the reversed Hall effect. Given that all these modifications are certainly of importance for understanding of many basic phenomena in astrophysical and space physics research, charged dust also provides a new tool to affect plasma structures in various laboratory and fusion devices.

This work was supported by the Deutsche Forschungsgemeinschaft (DFG) under the Grant No. YA 349/1-1 (Special Program, PlanetMag, SPP 1488).

- <sup>1</sup>V. Rozhansky, "Mechanisms of transverse conductivity and generation of self-consistent electric fields in strongly ionized magnetized plasma," *Rev. Plasma Phys.* **24**, 1–52 (2008).
- <sup>2</sup>H. Volland, *Atmospheric Electrodynamics* (Springer, Berlin/Heidelberg, 1984).
- <sup>3</sup>M. J. Rycroft and R. G. Harrison, *Space Sci. Rev.* **168**, 363 (2012).
- <sup>4</sup>A. Brekke, *Physics of the Upper Polar Atmosphere* (Wiley, Hoboken, NJ, 1997).
- <sup>5</sup>R. A. Treumann and W. Baumjohann, *Front. Phys.: Space Phys.* **1**, 31 (2013).
- <sup>6</sup>A. Lazarian, G. Eyink, E. Vishniac, and G. Kowal, "Magnetic reconnection in astrophysical environments," in *Magnetic Fields in Diffuse Media*, Astrophysics and Space Science Library, edited by A. Lazarian, E. M. de Gouveia Dal Pino, and C. Melioli (Springer-Verlag, Berlin/Heidelberg, 2015), Vol. 407, pp. 311–372.
- <sup>7</sup>V. E. Fortov, A. G. Khrapak, S. A. Khrapak, V. I. Molotkov, and O. F. Petrov, *Phys. Usp.* **47**, 447 (2004).
- <sup>8</sup>C. K. Goertz, *Rev. Geophys.* **27**, 271, <https://doi.org/10.1029/RG027i002p00271> (1989).
- <sup>9</sup>S. Simon, J. Saur, H. Kriegel, F. M. Neubauer, U. Motschmann, and M. K. Dougherty, *J. Geophys. Res.* **116**, A04221, <https://doi.org/10.1029/2011JA016842> (2011).
- <sup>10</sup>H. Kriegel, S. Simon, U. Motschmann, J. Saur, F. M. Neubauer, A. M. Persoon, M. K. Dougherty, and D. A. Gurnett, *J. Geophys. Res.* **116**, A10223, <https://doi.org/10.1029/2011JA016842> (2011).
- <sup>11</sup>H. Kriegel, S. Simon, P. Meier, U. Motschmann, J. Saur, A. Wennmacher, D. F. Strobel, and M. K. Dougherty, *J. Geophys. Res.* **119**, 2740, <https://doi.org/10.1002/2013JA019440> (2014).
- <sup>12</sup>V. V. Yaroshenko and H. Lühr, *Plasma Phys. Controlled Fusion* **58**, 014010 (2016).
- <sup>13</sup>V. V. Yaroshenko and H. Lühr, *Icarus* **278**, 79 (2016).
- <sup>14</sup>T. W. Hill, M. F. Thomsen, R. L. Tokar, A. J. Coates, G. R. Lewis, D. T. Young, F. J. Crary, R. A. Baragiola, R. E. Johnson, Y. Dong, R. J. Wilson, G. H. Jones, J.-E. Wahlund, D. G. Mitchell, and M. Horányi, *J. Geophys. Res.* **117**, A05209, <https://doi.org/10.1029/2011JA017218> (2012).
- <sup>15</sup>M. Wardle and C. Ng, *Mon. Not. R. Astron. Soc.* **303**, 239 (1999).
- <sup>16</sup>M. Wardle, *Astrophys. Space Sci.* **292**, 317 (2004).
- <sup>17</sup>M. Wardle and R. Salmeron, *Mon. Not. R. Astron. Soc.* **422**, 2737 (2012).
- <sup>18</sup>A. M. Zadorozhny, "Effects of charged dust on mesospheric electrical structure," *Adv. Space Res.* **28**, 1059 (2001).
- <sup>19</sup>E. Thomas, Jr., R. L. Merlino, and M. Rosenberg, *IEEE Trans. Plasma Sci.* **41**, 811 (2013).
- <sup>20</sup>E. Thomas, U. Konopka, B. Lynch, S. Adams, S. LeBlanc, R. L. Merlino, and M. Rosenberg, *Phys. Plasmas* **22**, 113708 (2015).
- <sup>21</sup>M. Rapp and F.-J. Lübken, *Atmos. Chem. Phys.* **4**, 2601 (2004).
- <sup>22</sup>J. S. Mathis, W. Rumpl, and K. H. Nordsieck, *Astrophys. J.* **217**, 425 (1977).
- <sup>23</sup>V. Yaroshenko, S. Khrapak, H. Thomas, and G. Morfill, *Phys. Plasmas* **19**, 023702 (2012).
- <sup>24</sup>S. A. Khrapak, A. V. Ivlev, G. E. Morfill, and H. M. Thomas, *Phys. Rev. E* **66**, 046414 (2002).
- <sup>25</sup>B. D. Teolis, M. E. Perry, B. A. Magee, J. Westlake, and J. H. Waite, *J. Geophys. Res.* **115**, A09222, <https://doi.org/10.1029/2009JA015192> (2010).
- <sup>26</sup>M. W. Morooka, J.-E. Wahlund, A. I. Eriksson, W. M. Farrell, D. A. Gurnett, W. S. Kurth, A. M. Persoon, M. Shafiq, M. André, and M. K. G. Holmberg, *J. Geophys. Res.* **116**, A12221, <https://doi.org/10.1029/2011JA017038> (2011).
- <sup>27</sup>T. A. Cassidy and R. E. Johnson, *Icarus* **209**, 696 (2010).
- <sup>28</sup>V. V. Yaroshenko, H. Lühr, and W. J. Miloch, *J. Geophys. Res. Space Phys.* **119**, 221, <https://doi.org/10.1002/2013JA019213> (2014).
- <sup>29</sup>V. V. Yaroshenko and H. Lühr, *J. Geophys. Res. Space Phys.* **119**, 6190, <https://doi.org/10.1002/2014JA020008> (2014).
- <sup>30</sup>B. T. Draine and H. M. Lee, *Astrophys. J.* **285**, 89 (1984).
- <sup>31</sup>R. Nishi, T. Nakano, and T. Umeyayashi, *Astrophys. J.* **368**, 181 (1991).